Cell PRESS
Cancer Cell
Article

# Akt Determines Replicative Senescence and Oxidative or Oncogenic Premature Senescence and Sensitizes Cells to Oxidative Apoptosis

Veronique Nogueira,[1] Youngkyu Park,[1] Chia-Chen Chen,[1] Pei-Zhang Xu,[1] Mei-Ling Chen,[1] Ivana Tonic,[1] Terry Unterman,[2,3] and Nissim Hay[1,*]
[1]Department of Biochemistry and Molecular Genetics
[2]Department of Medicine
University of Illinois at Chicago, Chicago, IL 60607, USA
[3]Jesse Brown VA Medical Center, Chicago, IL 60612, USA
*Correspondence: nhay@uic.edu
DOI 10.1016/j.ccr.2008.11.003

## SUMMARY

**Akt deficiency causes resistance to replicative senescence, to oxidative stress- and oncogenic Ras-induced premature senescence, and to reactive oxygen species (ROS)-mediated apoptosis. Akt activation induces premature senescence and sensitizes cells to ROS-mediated apoptosis by increasing intracellular ROS through increased oxygen consumption and by inhibiting the expression of ROS scavengers downstream of FoxO, particularly *sestrin 3*. This uncovers an Achilles' heel of Akt, since in contrast to its ability to inhibit apoptosis induced by multiple apoptotic stimuli, Akt could not inhibit ROS-mediated apoptosis. Furthermore, treatment with rapamycin that led to further Akt activation and resistance to etoposide hypersensitized cancer cells to ROS-mediated apoptosis. Given that rapamycin alone is mainly cytostatic, this constitutes a strategy for cancer therapy that selectively eradicates cancer cells via Akt activation.**

## INTRODUCTION

The serine/threonine kinase Akt is activated by extracellular signals that activate phosphatidylinositol 3-kinase (PI3K), which generates $PI(3,4,5)P_3$ ($PIP_3$). Akt activity is negatively regulated by phospholipid phosphatases that negate the activity of PI3K, such as the tumor suppressor PTEN. In mammalian cells, there are three separate genes encoding the three mammalian Akt isoforms (Akt1–3). Akt activity is also downregulated by activation of its downstream effector mTORC1, which in turn induces a negative feedback mechanism that inhibits Akt activity (reviewed in Bhaskar and Hay, 2007).

Hyperactivated Akt both provides protection from apoptosis and promotes uncontrolled cell-cycle progression (Kandel et al., 2002), two major prerequisites for cancer susceptibility, and this may explain, at least in part, its frequent activation in human cancers (reviewed in Bhaskar and Hay, 2007). However, the most evolutionarily conserved function of Akt is in the control of energy metabolism, which in mammalian cells is coupled to its ability to inhibit apoptosis and to promote cell-cycle progression (reviewed in Plas and Thompson, 2005; Robey and Hay, 2006).

The coupling between energy metabolism and life span is well documented, and calorie restriction has been shown to extend life span in a wide spectrum of organisms. Attenuated insulin signaling through PI3K and its downstream effector, Akt, is associated with a decline in energy metabolism and an increase in life span. In *C. elegans*, increased life span associated with impaired PI3K/Akt signaling requires the presence of the forkhead transcription factor DAF-16. There are four mammalian homologs of DAF-16: FOXO1, FOXO3a, FOXO4, and FOXO6 (Greer and Brunet, 2005). Akt directly phosphorylates DAF-16 and its mammalian homologs, and this phosphorylation excludes them from

## SIGNIFICANCE

Oncogenic and oxidative stress-induced senescence attenuates tumorigenesis. Here we show that Akt mediates this premature senescence. Akt exerts its effects on senescence by elevating intracellular reactive oxygen species (ROS). The elevation of ROS induced by Akt also sensitizes cells to ROS-mediated cell death and can therefore be exploited for cancer therapy. Hyperactivation of Akt, which occurs frequently in human cancers, promotes resistance to chemotherapy. Here we provide a strategy that not only evades chemoresistance induced by Akt but also selectively eradicate cancer cells that display hyperactive Akt. As a proof of concept for this strategy, we show that a ROS inducer preferentially suppresses in vivo tumor growth of cancer cells expressing activated Akt, which is further accelerated by rapamycin.

the nucleus, thereby inhibiting their transcriptional activity (Greer and Brunet, 2005). Thus, the activity of DAF-16 and its mammalian homologs is increased when Akt activity is reduced.

The accumulation of somatic damage is considered a major determinant of life span at both the organismal and cellular levels. This damage is caused mainly by the accumulation of reactive oxygen species (ROS) (Chance et al., 1979), which are natural byproducts of oxidative energy metabolism. Damage induced by ROS, including DNA lesions, protein oxidation, and lipid peroxidation, is determined by both the rate of energy metabolism and the activity of ROS scavengers such as superoxide dismutase (SOD) and catalase that degrade hydrogen peroxide. Multiple experiments have shown that ROS play a critical role in determining life span and cellular senescence in mammalian cells (reviewed in Balaban et al., 2005). The senescence of mouse embryonic fibroblasts (MEFs), which have long telomeres, is likely to occur via accumulation of ROS when grown at ambient oxygen levels (Parrinello et al., 2003). Consistently, earlier observations showed that human diploid cells undergo senescence at a lower rate under low-oxygen conditions (Packer and Fuehr, 1977).

Here we provide genetic evidence that Akt determines replicative senescence of mammalian cells in culture and mediates premature senescence induced by activated Ras or oxidative stress. Additionally, Akt activation is sufficient to induce premature senescence. In the course of these studies, we found that Akt also sensitizes cells to ROS-mediated apoptosis. We showed that Akt exerts its effect by increasing intracellular levels of ROS through an increase in oxygen consumption and the inhibition of FoxO transcription factors.

Despite its ability to inhibit apoptosis, Akt could not protect against ROS-mediated cell death but rather sensitized cells to this cell death. Thus, we uncovered the Achilles' heel of Akt, which can be exploited for cancer therapy to selectively kill cancer cells with hyperactive Akt. Most importantly, we showed that rapamycin, which is usually cytostatic, sensitizes cells to ROS-mediated cell death because it also activates Akt via the inhibition of a negative feedback loop (Bhaskar and Hay, 2007; Harrington et al., 2005; Hay, 2005). Thus, by combining rapamycin and a ROS inducer, it is possible not only to evade chemoresistance mediated by Akt activation but also to selectively kill cancer cells with hyperactive Akt. In addition, our demonstration that rapamycin-treated cells are sensitized to ROS-induced cell death provides a strategy that would substantially increase the efficacy of rapamycin treatment.

## RESULTS

### Akt Regulates Cellular Life Span

We used wild-type (WT) or Akt1 and Akt2 double-knockout (Akt1/2 DKO) MEFs to determine the role of Akt in the regulation of cellular life span. MEFs were subjected to 3T3 protocol to calculate population doubling level (PDL). Senescence-associated β-galactosidase (SA-β-Gal) staining and bromodeoxyuridine (BrdU) incorporation were used as readouts for senescence. As shown in Figure 1A, WT MEFs began senescing after passage 13, whereas Akt1/2 DKO MEFs began senescing after passage 16. This was also confirmed by the cells' enlarged and flattened cell morphology (data not shown), by SA-β-Gal staining (Figure 1B), and by BrdU incorporation (Figure 1C). Notably, we have previously shown that Akt1/2 DKO cells divide more slowly than WT cells (Skeen et al., 2006); therefore, we passaged the cells every 5 days instead of every 3 days. As shown in Figure 1D, the senescence of Akt1/2 DKO still lagged behind WT MEFs. These results provided evidence that Akt determines the cellular life span and replicative senescence of MEFs.

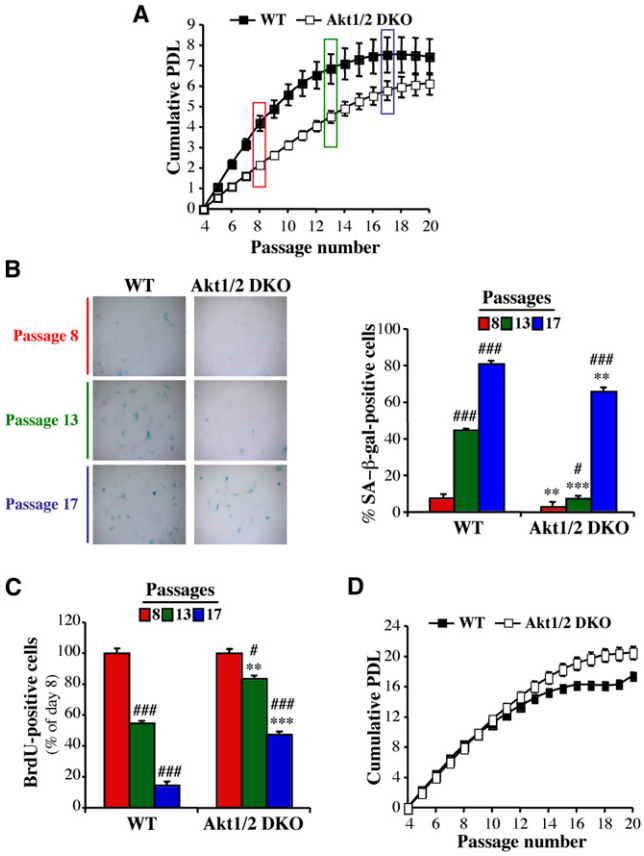


**Figure 1. Akt Regulates Replicative Senescence**

(A) Cells were subjected to the 3T3 protocol as described in Experimental Procedures. Cells were counted at each passage every 3 days, and the population doubling level (PDL) was calculated for wild-type (WT) and Akt1/2 null (Akt1/2 DKO) primary mouse embryonic fibroblasts (MEFs). Data represent the mean ± SEM of three independent experiments.

(B) Primary MEFs were stained for senescence-associated β-galactosidase (SA-β-Gal) activity at passage 8 (before visible signs of senescence), at passage 13 (when WT cells began to exhibit proliferative arrest), and at passage 17 (when Akt1/2 DKO cells began to exhibit proliferative arrest). Left: representative photographic images of cells stained for SA-β-Gal activity at passages 8, 13, and 17. Right: SA-β-Gal-positive cells were counted in at least five fields of triplicate plates. Data represent the mean ± SEM of three independent experiments. $^{**}p < 0.01$, $^{***}p < 0.001$ versus WT; #$p < 0.05$, ###$p < 0.001$ versus passage 8.

(C) Proliferation rate of primary MEFs as measured by BrdU labeling for 24 hr prior to fixation and staining. BrdU incorporation was carried out as described in Experimental Procedures and determined by counting at least 150 cells from at least five fields in triplicate plates. Data represent the mean ± SEM of three independent experiments. $^{**}p < 0.01$, $^{***}p < 0.001$ versus WT; #$p < 0.05$, ###$p < 0.001$ versus passage 8.

(D) Cumulative PDL of WT and Akt1/2 DKO primary MEFs as described in (A), except that cells were split and counted every 5 days. Data represent the mean ± SEM of at least three independent experiments.

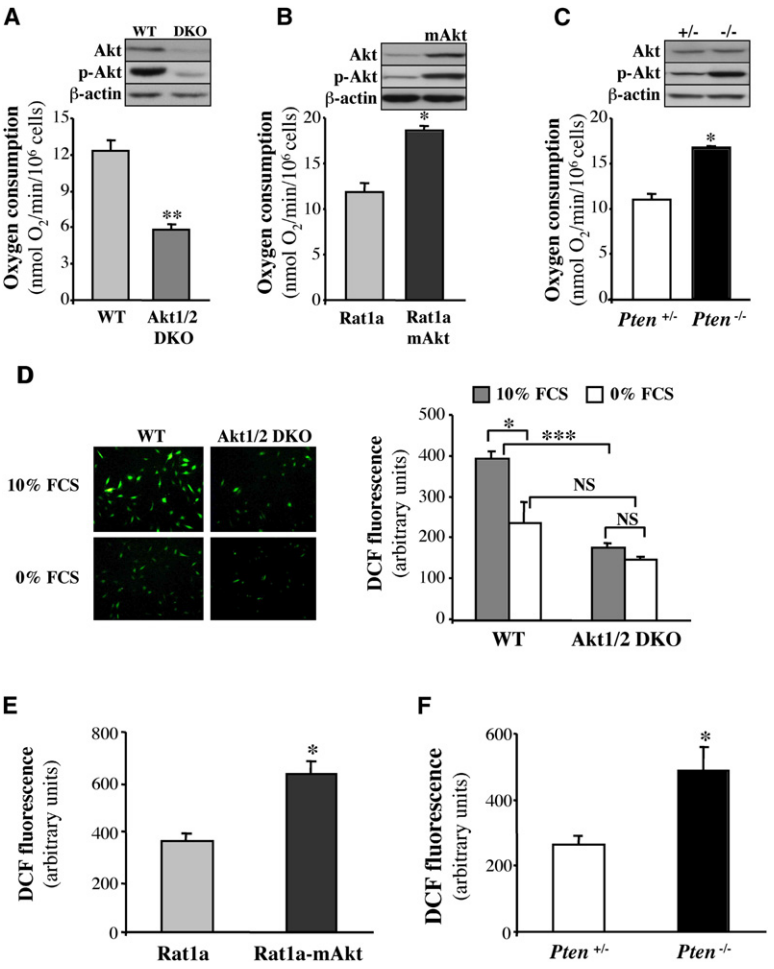


**Figure 2. Akt Regulates Oxygen Consumption and Reactive Oxygen Species Generation**

(A–C) Rates of oxygen consumption in WT or Akt1/2 DKO MEFs (A), Rat1a cells or Rat1a cells expressing activated Akt (Rat1a-mAkt) (B), and *Pten*$^{+/-}$ or *Pten*$^{-/-}$ MEFs (C) were measured as described in Experimental Procedures. Immunoblots show the relative levels of phosphorylated Akt (p-Akt Ser473) and total Akt in all cell lines. *p < 0.05, **p < 0.01 versus WT (A), Rat1a (B), and *Pten*$^{+/-}$ (C).

(D–F) Akt mediates the generation of reactive oxygen species (ROS). Data are expressed as arbitrary units after being normalized to protein concentration.

(D) ROS levels in WT and Akt1/2 DKO MEFs incubated in 10% FBS or in 0% FBS overnight. Left: representative images of cells stained with dichlorofluorescein (DCF). Right: quantification of ROS levels. *p < 0.05, ***p < 0.001; NS, not significant.

(E) ROS levels in Rat1a and Rat1a-mAkt cells. *p < 0.05 versus Rat1a.

(F) ROS levels in *Pten*$^{+/-}$ and *Pten*$^{-/-}$ MEFs. *p < 0.05 versus *Pten*$^{+/-}$.

All data represent the mean ± SEM of at least three independent experiments.

The results obtained with MEFs were corroborated using human foreskin diploid fibroblasts (HDFs). The knockdown of Akt1 alone in HDFs minimally impaired proliferation rate but markedly attenuated cellular senescence as measured by population doublings (see Figure S1A available online).

## Akt Regulates Cellular Life Span and Intracellular ROS Levels by Mediating Oxygen Consumption and Inhibiting FoxO Transcription Factors

Life span in culture of MEFs, and to some extent HDFs, is coupled to oxygen consumption and intracellular ROS (Parrinello et al., 2003). We therefore determined the role of Akt in these two parameters. Oxygen consumption was impaired in Akt1/2 DKO cells (Figure 2A) and was accelerated in cells expressing activated Akt (Figure 2B) and in *Pten*$^{-/-}$ cells (Figure 2C). We next determined whether Akt could affect intracellular levels of ROS and found that Akt1/2 DKO MEFs had significantly lower ROS levels compared with WT MEFs (Figure 2D), whereas cells expressing activated Akt (Figure 2E) and *Pten*$^{-/-}$ cells (Figure 2F) had significantly higher levels of ROS. These results indicated that Akt regulates intracellular ROS levels. We had previously shown that activation of Akt increases ATP production by both glycolysis and oxidative phosphorylation (Gottlob et al., 2001). Because ROS are byproducts of oxidative phosphorylation, Akt-induced ROS levels could be dependent in part on Akt-mediated oxygen consumption. To show that the decrease in oxygen consumption in Akt1/2 DKO MEFs correlates with a decrease in ROS production, we substituted glucose with galactose in the cell culture media. This substitution decreases the generation of ATP from glycolysis, forcing cells to increase respiration (Rossignol et al., 2004; Warburg et al., 1967). Indeed, the substitution of glucose with galactose increased oxygen consumption in Akt1/2 DKO MEFs, with concomitant increase in ROS generation (Figures S2A and S2B). These results provided indirect evidence suggesting that the decrease in oxygen consumption in Akt1/2 DKO MEFs contributes to the reduced ROS levels.

To exclude the possibility that the reduced ROS levels observed in Akt1/2 DKO MEFs were due to the decrease in their proliferation rate, we immortalized both WT and Akt1/2 DKO MEFs with SV40 large T. The SV40 large T-immortalized WT and Akt1/2 DKO MEFs proliferated at a similar rate (Figure S2C), yet the Akt1/2 DKO MEFs still displayed decreased oxygen consumption and ROS levels (Figures S2D and S2E). Also, when WT and Akt1/2 DKO MEFs were grown to confluency and stopped dividing (Figure S2F), oxygen consumption and ROS levels remained reduced in the Akt1/2 DKO MEFs (Figures S2G and S2H). These results indicated that the reduced ROS levels in Akt1/2 DKO MEFs are not a consequence of their attenuated proliferation.

Because FoxO transcription factors are downstream effectors of Akt and have a conserved role in ROS regulation via the regulation of detoxifying enzymes (Greer and Brunet, 2005), we examined the contribution of FoxO to the reduced ROS levels in Akt1/2 DKO MEFs. FoxO transcriptional activity was elevated in Akt1/2 DKO MEFs (Figure S3). Consistently, levels of both manganese superoxide dismutase (MnSOD) and catalase, two known targets of FoxO (Kops et al., 2002; Nemoto and Finkel, 2002), were elevated in Akt1/2 DKO MEFs (Figure 3A). Moreover, when

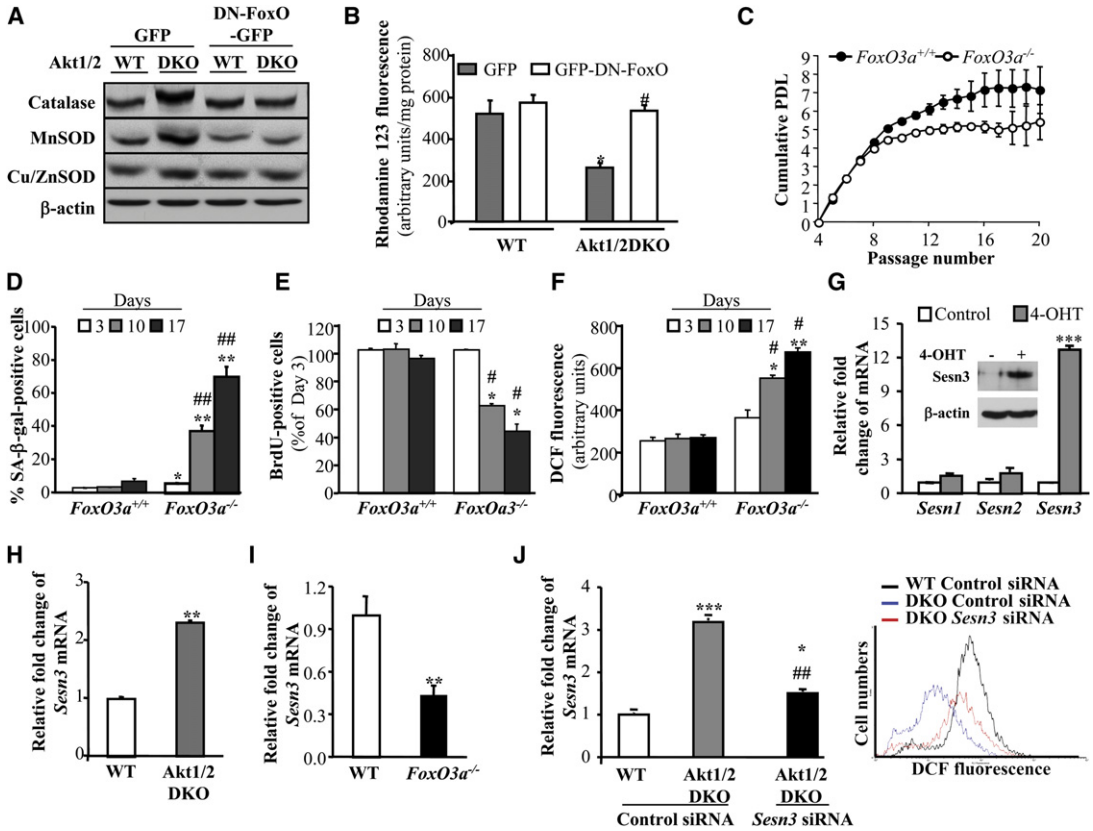


**Figure 3. FoxO Transcription Factors Regulate the Generation of ROS and Replicative Senescence Downstream of Akt**

(A) Catalase and manganese superoxide dismutase (MnSOD) are upregulated in Akt1/2 DKO MEFs and are downregulated by dominant-negative FoxO1 (DN-FoxO). The generation of cells expressing DN-FoxO is described in Experimental Procedures. Proteins extracted from exponentially growing DN-p53-immortalized WT and Akt1/2 DKO MEFs overexpressing GFP (control vector) or DN-FoxO-GFP were subjected to immunoblotting using antibodies specific for catalase, MnSOD, Cu/ZnSOD, or β-actin as a loading control.

(B) DN-FoxO restores intracellular levels of ROS in Akt1/2 DKO cells. ROS were quantified in WT and Akt1/2 DKO MEFs overexpressing GFP or DN-FoxO-GFP after incubation of cells with rhodamine 123 as a sensor of ROS production (described in Experimental Procedures). Data represent the mean ± SEM of three independent experiments. *p < 0.05 versus GFP-WT; #p < 0.05 versus GFP-Akt1/2 DKO.

(C) Wild-type (*FoxO3a*$^{+/+}$) and *FoxO3a* null (*FoxO3a*$^{-/-}$) primary MEFs were analyzed for replicative senescence using the 3T3 protocol. Data represent the mean ± SEM of three independent experiments.

(D) SA-β-Gal activity in primary *FoxO3a*$^{+/+}$ and *FoxO3a*$^{-/-}$ cells. Assay was performed at 3, 10, and 17 days in culture. *p < 0.05, **p < 0.01 versus *FoxO3a*$^{+/+}$; ##p < 0.01 versus day 3. Data represent the mean ± SEM of three independent experiments.

(E) Cell proliferation was assessed by BrdU incorporation at the time points in (D). *p < 0.05 versus *FoxO3a*$^{+/+}$; #p < 0.05 versus day 3. Data represent the mean ± SEM of three independent experiments.

(F) Level of ROS in primary *FoxO3a*$^{+/+}$ and *FoxO3a*$^{-/-}$ cells at the time points in (D). Data are presented as arbitrary units after being normalized to protein concentration. *p < 0.05, **p < 0.01 versus *FoxO3a*$^{+/+}$; #p < 0.05 versus day 3. Data represent the mean ± SEM of at least three independent experiments.

(G) Levels of *Sesn1*, *Sesn2*, and *Sesn3* mRNA as determined by quantitative RT-PCR. WT MEFs immortalized with DN-p53 and stably expressing FoxO1AAA-ER were treated with 4-hydroxytamoxifen (4-OHT) followed by RNA analysis as described in Supplemental Experimental Procedures. ***p < 0.001 versus control. Inset: immunoblot showing induction of Sesn3 protein level after FoxO1AAA-ER activation by 4-OHT.

(H) Level of *Sesn3* mRNA in WT and Akt1/2 DKO MEFs immortalized with DN-p53, as assessed by quantitative RT-PCR. **p < 0.01 versus WT. Data represent the mean ± SEM of three independent experiments.

(I) Level of *Sesn3* mRNA in WT and *FoxO3a*$^{-/-}$ MEFs immortalized with DN-p53. All RNA analyses were performed in triplicates. **p < 0.001 versus WT. Data represent the mean ± SEM of three independent experiments.

(J) Knockdown of *Sesn3* in Akt1/2 DKO MEFs elevates ROS levels to those in WT cells. Left: levels of *Sesn3* mRNA in WT, Akt1/2 DKO, and Akt1/2 DKO-SESN3 KD MEFs as assessed by quantitative RT-PCR. *p < 0.05, ***p < 0.001 versus control siRNA in WT; ##p < 0.01 versus control siRNA in Akt1/2 DKO. Data represent the mean ± SEM of three independent experiments. Right: levels of ROS in WT, Akt1/2 DKO, and Akt1/2 DKO-SESN3 KD MEFs as assessed by DCF fluorescence.

dominant-negative FoxO1 (DN-FoxO), containing only its DNA-binding domain, was expressed in Akt1/2 DKO cells, MnSOD and catalase levels were reduced to their levels in WT cells, although we did not find a further decrease in the levels of these enzymes in WT cells expressing DN-FoxO. Importantly, we identified an additional mechanism by which FoxOs could affect intracellular ROS levels. We found that sestrin 3 (*Sesn3*) expression was highly induced by activated FoxO (Figure 3G). The ability of FoxO to elevate *Sesn3* RNA and protein is conserved in rodent and human cells (C.-C.C. and N.H, unpublished data). Sesn3 is

a member of a family of proteins that also includes sestrin1 (Sesn1) and sestrin2 (Sesn2). All three members have been shown to decrease intracellular ROS and to confer resistance to oxidative stress (Kopnin et al., 2007), probably by regenerating overoxidized peroxiredoxins that deoxidize ROS (Budanov et al., 2004). *Sesn1* and *Sesn2* are p53 target genes and are responsible for the resistance to oxidative stress induced by p53 both in vitro and in vivo (Budanov et al., 2002; Matheu et al., 2007; Sablina et al., 2005). *Sesn3* expression is not regulated by p53, but its overexpression has been shown to reduce ROS induced by activated Ras (Kopnin et al., 2007). Therefore, FoxO-induced *Sesn3* expression could contribute to the regulation of intracellular ROS and to resistance to oxidative stress. Indeed, we found that *Sesn3* expression was elevated in Akt1/2 DKO MEFs (Figure 3H) and was reduced in *FoxO3a*$^{-/-}$ MEFs (Figure 3I). Furthermore, the knockdown of *Sesn3* in Akt1/2 DKO cells restored ROS levels to the levels observed in WT cells (Figure 3J). These results suggest that Sesn3 is a major regulator of intracellular ROS downstream of Akt and FoxOs. Since all of the MEFs used in these studies were immortalized with DN-p53, the effect of FoxO and Akt on *Sesn3* expression is clearly p53 independent. Consistent with ability of FoxO to elevate the expression of ROS scavengers in Akt1/2 DKO MEFs, we found that DN-FoxO restored ROS levels in Akt1/2 DKO MEFs (Figure 3B).

To further assess the role of FoxO in the regulation of life span in culture, we utilized *FoxO3a* null MEFs, as FoxO3a is the major FoxO isoform expressed in MEFs (data not shown). By following replicative senescence of primary WT and *FoxO3a*$^{-/-}$ MEFs, it was evident that *FoxO3a*$^{-/-}$ MEFs senesced much faster than WT MEFs (Figure 3C). Furthermore, we found that *FoxO3a*$^{-/-}$ MEFs senesced spontaneously after a few days in culture. When *FoxO3a*$^{-/-}$ MEFs were plated at low density and were allowed to grow for 17 days, they underwent senescence, whereas WT cells did not senesce (Figures 3D and 3E). This was correlated with the accumulation of ROS in *FoxO3a*$^{-/-}$ cells when compared with WT cells (Figure 3F).

## Akt Deficiency Exerts Resistance to Premature Senescence Induced by Oxidative Stress and by Activated Ras

Having determined the role of Akt and FoxO in replicative senescence, we sought to determine the role of Akt in premature senescence induced by oxidative stress. We first examined the ability of WT and Akt1/2 DKO primary MEFs to senesce upon exposure to $H_2O_2$. Exposure to sublethal concentrations of $H_2O_2$ increased intracellular levels of ROS in WT MEFs (Figure 4A) and decreased life span in culture as assessed by enlarged and flattened cell morphology, SA-β-Gal staining (Figure 4B), and BrdU incorporation (Figure 4C). In Akt1/2 DKO MEFs, however, ROS levels were markedly lower upon exposure to $H_2O_2$ (Figure 4A), and likewise, Akt1/2 DKO MEFs were markedly resistant to premature senescence as compared with WT MEFs (Figures 4B and 4C). Notably, intracellular ROS levels continued to increase after $H_2O_2$ treatment (Figure 4A); this is probably due to the activation of Akt by $H_2O_2$ (see below). The requirement of Akt for oxidative stress-induced senescence was also corroborated in HDFs (Figures S1B and S1C).

The resistance of Akt1/2 DKO MEFs to oxidative stress-induced senescence was abrogated by the overexpression of DN-FoxO or the knockdown of *FoxO3a* (Figures S4A–S4C). Furthermore, the knockdown of *Sesn3*, which is a FoxO target (Figures 3G–3I), abrogated the resistance of Akt1/2 DKO MEFs to oxidative stress-induced premature senescence (Figure 4D). Conversely, expression of activated FoxO1 in *p27*$^{-/-}$ MEFs conferred relative resistance to premature senescence (Figures S4D and S4E). For this experiment, we used *p27*$^{-/-}$ cells to avoid cell-cycle arrest induced by activated FoxO (Greer and Brunet, 2005). Similar results were obtained when *p27*$^{-/-}$ MEFs were compared with *Akt1*$^{-/-}$*p27*$^{-/-}$ MEFs (Figures S4F–S4H). The deficiency of Akt1 in *p27*$^{-/-}$ cells was sufficient to exert resistance to $H_2O_2$-induced senescence, although to a lesser extent than observed when both *Akt1* and *Akt2* were deleted in the WT background. Activated FoxO reduced ROS levels and exerted resistance to $H_2O_2$-induced senescence in *p27*$^{-/-}$ MEFs similar to that observed in *Akt1*$^{-/-}$*p27*$^{-/-}$ MEFs in the absence of activated FoxO (Figures S4F–S4H).

Oncogenic Ras induces premature senescence of primary cells (Serrano et al., 1997), which has been shown to be mediated at least in part via elevated intracellular ROS levels (Lee et al., 1999). We therefore examined the ability of activated Ras (H-Ras$^{V12}$) to induce senescence in Akt-deficient cells. As expected, activated Ras elevated ROS levels in WT cells, but this elevation was markedly reduced in Akt1/2 DKO MEFs (Figure 4E). Expression of DN-FoxO in Akt1/2 DKO MEFs increased ROS levels that were induced by activated Ras (Figure S5A). Consistent with previous results (Lee et al., 1999), Ras-induced premature senescence was preceded by reduced MnSOD levels (Figure S5B) and was inhibited by the antioxidant N-acetyl-L-cysteine (NAC) (Figures S5C and S5D). Accordingly, Akt1/2 DKO MEFs were relatively resistant to premature senescence induced by activated Ras (Figures 4F and 4G).

Premature senescence induced by activated Ras is dependent on p53 activation and the increase in p19$^{ARF}$ and p16 (reviewed in Schmitt, 2007). We therefore analyzed p53 activation and p19$^{ARF}$ and p16 levels, as assessed by serine 15 phosphorylation of p53, in WT and Akt1/2 DKO MEFs following activated Ras expression (Figure 4H) or exposure to $H_2O_2$ (Figure 4I). As expected, p19$^{ARF}$ expression was elevated with concomitant activation of p53 and induction in p16 levels in WT cells, but these were substantially diminished in Akt1/2 DKO cells. Conversely, the activation of Akt, which is sufficient to induce premature senescence (Figures 5E and 5F), elevated the phosphorylation of p53 and the expression of p19$^{ARF}$ and p16, which were diminished in the presence of NAC (Figure S5I). Thus, Akt deficiency inhibits p53 phosphorylation and the induction of p19$^{ARF}$ and p16 by activated Ras or oxidative stress, while the activation of Akt is sufficient to induce p19$^{ARF}$ and p16, p53 phosphorylation, and premature senescence.

The resistance of Akt1/2 DKO MEFs to premature senescence induced by activated Ras was also dependent on FoxO, because activated FoxO1 increased this resistance in WT MEFs (Figures S5E and S5F). Consistently, we found that *FoxO3a*$^{-/-}$ MEFs were hypersensitized to premature senescence induced by $H_2O_2$ or activated Ras (Figures 5A–5D).

Taken together, these results provide compelling evidence that both oxidative stress- and activated Ras-induced premature senescence are dependent on Akt, which exerts its effects via an

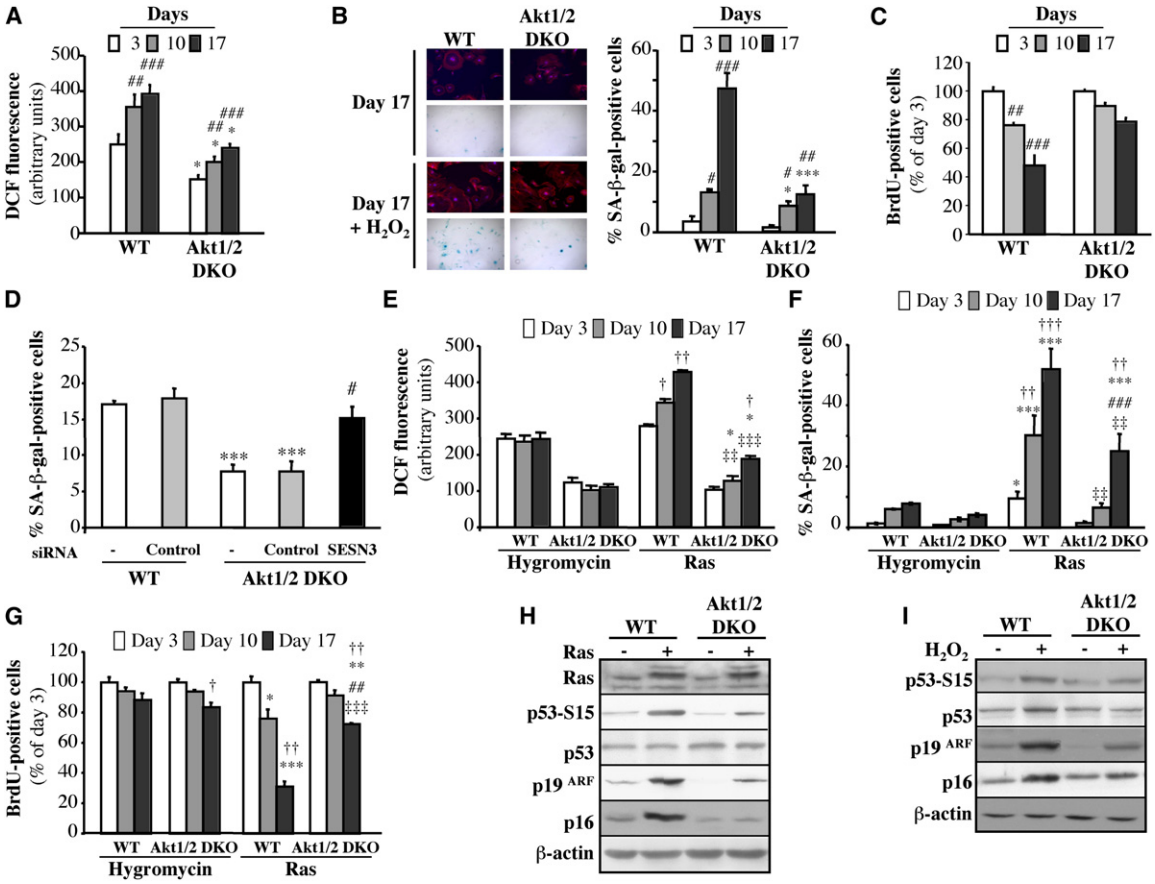


**Figure 4. Akt Deficiency Exerts Resistance to $H_2O_2$- and Ras-Induced Premature Senescence**

(A–C) Premature senescence of primary WT and Akt1/2 DKO MEFs was induced with 75 μM $H_2O_2$ as described in Experimental Procedures. At days 3, 10, and 17 after treatment, cells were analyzed for ROS production (A), SA-β-Gal activity (B), and BrdU incorporation (C). In (B), left panel shows representative images of cells stained for F-actin/DAPI (fluorescence) and SA-β-Gal activity (bright-field) at day 17, and right panel shows quantification of SA-β-Gal-positive cells. *p < 0.05, ***p < 0.001 versus WT; #p < 0.05, ##p < 0.01 ###, p < 0.001 versus day 3.

(D) Knockdown of *Sesn3* overrides the resistance of Akt1/2 DKO MEFs to $H_2O_2$-induced senescence. Premature senescence of primary WT and Akt1/2 DKO MEFs was induced with 75 μM $H_2O_2$ as described in Experimental Procedures, and at day 0, cells were transfected with siRNAs. Cells were then analyzed for SA-β-Gal activity at day 7 posttransfection. ***p < 0.001 versus WT; #p < 0.05 versus Akt1/2 DKO.

(E–G) Primary WT and Akt1/2 DKO MEFs were infected with empty vector (hygromycin) or H-$Ras^{V12}$-expressing retroviruses. At days 3, 10, and 17 postselection (see Experimental Procedures), the cells were analyzed for ROS production (E), SA-β-Gal activity (F), and BrdU incorporation (G). *p < 0.05, **p < 0.01, ***p < 0.001 versus WT-Hygro; ##p < 0.01, ###p < 0.001 versus Akt1/2 DKO-Hygro; ‡‡p < 0.01, ‡‡‡p < 0.001 versus WT-Ras; †p < 0.05, ††p < 0.01, †††p < 0.001 versus day 3.

(H) Immunoblot showing expression of Ras, p53 phospho-Ser15, total p53, $p19^{ARF}$, and p16 following expression of H-$Ras^{V12}$ in WT or Akt1/2 DKO MEFs.

(I) Immunoblot showing expression of p53 phospho-Ser15, total p53, $p19^{ARF}$, and p16 following addition of $H_2O_2$ to WT or Akt1/2 DKO MEFs.

All data represent the mean ± SEM of at least three independent experiments.

increase in oxygen consumption and inhibition of FoxO transcription factors.

## Akt Sensitizes Cells to Oxidative Stress-Induced Cell Death—The Achilles' Heel of Akt

Exposure of immortalized MEFs expressing DN-p53 to increasing amounts of $H_2O_2$ induced cell death (Figure 6A). We expected that WT cells would be more resistant to apoptosis than Akt1/2 DKO cells. Indeed, Akt1/2 DKO cells were more sensitive than WT cells to etoposide-induced cell death (Figure S9A). Surprisingly, however, we found that Akt1/2 DKO cells were more resistant than WT cells to cell death induced by increasing concentrations of $H_2O_2$. The increased sensitivity of WT cells to $H_2O_2$-mediated cell death was likely due to the activation of Akt and the subsequent phosphorylation and inactivation of FoxO transcription factors, thereby downregulating detoxifying enzymes (Figure 6B). Oxidative stress leads to the activation of Akt either by inactivating PTEN (Leslie et al., 2003) or by the activation of $p66^{shc}$ (Nemoto and Finkel, 2002), or both. In the absence of Akt1 and Akt2, FoxO transcription factors were not significantly inhibited by $H_2O_2$, thereby maintaining relatively high levels of detoxifying enzymes (Figure 6B). Indeed, expression of DN-FoxO (Figure S6A) or knockdown of *FoxO3a* (Figure S6B) increased the susceptibility of Akt1/2 DKO MEFs to cell death, whereas expression of activated FoxO in $p27^{-/-}$ MEFs rendered them more resistant to

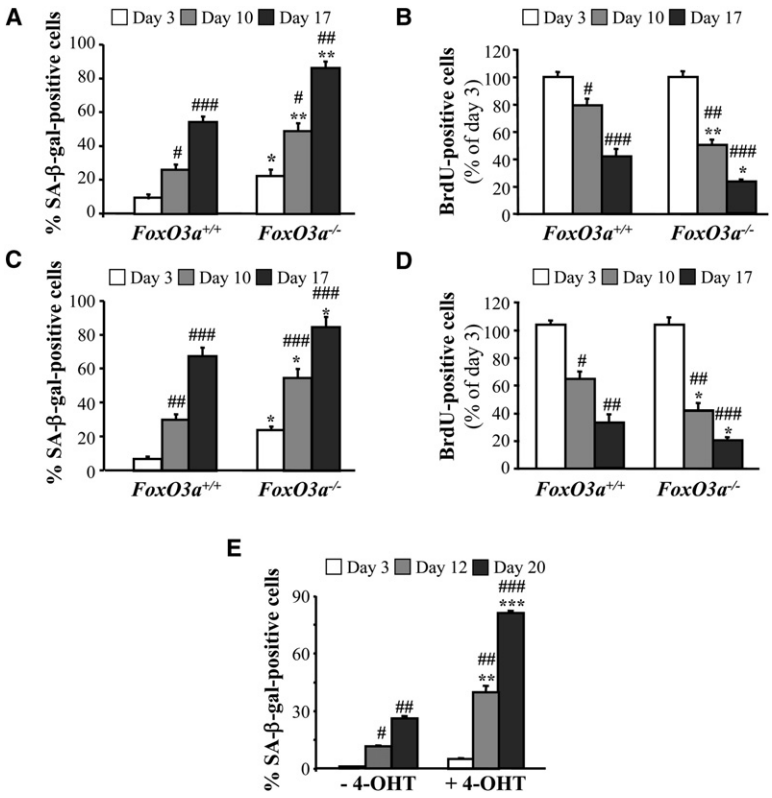


**Figure 5. *FoxO3a*$^{-/-}$ MEFs Are Sensitized to $H_2O_2$- and Ras-Induced Premature Senescence**

(A and B) Primary *FoxO3a*$^{+/+}$ and *FoxO3a*$^{-/-}$ MEFs were treated with 75 μM $H_2O_2$. At days 3, 10, and 17 posttreatment, cells were analyzed for SA-β-Gal activity (A) and BrdU incorporation (B).

(C and D) Primary *FoxO3a*$^{+/+}$ and *FoxO3a*$^{-/-}$ MEFs were infected with retrovirus expressing H-Ras$^{V12}$. At days 3, 10, and 17 postselection, cells were analyzed for SA-β-Gal activity (C) and BrdU incorporation (D). For (A)–(D), *p < 0.05, **p < 0.01 versus *FoxO3a*$^{+/+}$; #p < 0.05, ##p < 0.01, ###p < 0.001 versus day 3.

(E) Activated Akt induces premature senescence of MEFs. Primary WT MEFs were infected with retrovirus expressing inducible myristoylated Akt (mAkt-ER). After selection, cells were either left untreated or treated with 4-OHT. At days 3, 12, and 20 postincubation with 4-OHT, cells were analyzed for SA-β-Gal activity. **p < 0.01, ***p < 0.001 versus vehicle control; #p < 0.05, ##p < 0.01, ###p < 0.001 versus day 3. Data represent the mean ± SEM of at least three independent experiments.

$H_2O_2$-induced cell death (Figure S6C). Cells expressing activated Akt and *Pten*$^{-/-}$ cells were more susceptible to $H_2O_2$-induced death (Figures 6C and 6D). To determine whether scavengers of ROS, regulated by FoxO, are responsible at least in part for the resistance of Akt1/2 DKO MEFs to $H_2O_2$-induced cell death, we knocked down *Sesn3* expression in Akt1/2 DKO MEFs or overexpressed catalase in WT MEFs. Knockdown of *Sesn3* increased the sensitivity of Akt1/2 DKO MEFs to $H_2O_2$ (Figure S6D). Overexpression of catalase decreased the sensitivity of WT MEFs to $H_2O_2$ (Figure S6E), but not to the level observed in Akt1/2 DKO MEFs. These results suggest that multiple ROS scavengers induced by FoxO are responsible for the resistance of Akt1/2 DKO MEFs to $H_2O_2$-induced cell death.

Similar results were obtained when the cells were treated with β-phenylethyl isothiocyanate (PEITC), a natural compound found in consumable cruciferous vegetables that is known to increase intracellular ROS levels (Yu et al., 1998). Increasing amounts of PEITC were markedly less effective at killing Akt1/2 DKO cells than WT cells, whereas they were much more effective at killing *Pten*$^{-/-}$ cells than *Pten*$^{+/-}$ cells (Figures S7A and S7B). Similar results were observed with other rodent (Figure S7C) or human (Figure S7D) cells expressing activated Akt. We concluded that despite the ability of activated Akt to protect against cell death induced by a variety of stimuli, it cannot protect against ROS-induced cell death. Therefore, because Akt activation increases intracellular ROS levels and impairs ROS scavenging, it not only cannot protect from but also sensitizes to ROS-induced cell death. Thus, these observations uncovered the Achilles' heel of Akt.

## A Strategy to Selectively Eradicate Cancer Cells with Hyperactivated Akt by Inducing ROS in Combination with Rapamycin

Akt is frequently activated in human cancers (reviewed in Bhaskar and Hay, 2007; Hay, 2005) and thereby promotes resistance to therapeutic agents that induce apoptosis. Therefore, the hypersensitivity of activated Akt-expressing cells to ROS-induced cell death might be exploited to selectively eradicate and to overcome chemoresistance of cancer cells with hyperactivated Akt.

Rapamycin analogs, which are currently being used in clinical trials, are mostly cytostatic. One concern in using rapamycin analogs for cancer therapy is that they could also increase cell survival via the hyperactivation of Akt. This elevated Akt activity is due to the inhibition of the negative feedback loop induced by mTORC1 to inhibit Akt activity (reviewed in Bhaskar and Hay, 2007; Harrington et al., 2005; Hay, 2005). However, by activating Akt, rapamycin could further sensitize cells to ROS-induced cell death, and thus, the combination of rapamycin and oxidative stress might not only circumvent resistance to cell death but also selectively kill cells treated with rapamycin.

To explore this possibility, we first used rodent cells to provide a proof of concept. As shown in Figure S8, rapamycin alone did not induce cell death, but pretreatment with rapamycin augmented the ability of $H_2O_2$ to induce apoptosis. Although rapamycin treatment increased $H_2O_2$-induced apoptosis in both WT and Akt1/2 DKO cells, the level of WT cell apoptosis was significantly higher (Figure S8A). By contrast, rapamycin increased resistance to etoposide (Figures S9A). Furthermore, activated Akt-expressing cells were more sensitive than control cells to cell death induced by the combination of rapamycin and $H_2O_2$, (Figure S8B), indicating that this cell death is dependent on Akt activity. By contrast, cells expressing activated Akt were more resistant to etoposide, and rapamycin increased this resistance (Figure S9B). Next, we evaluated the effect of rapamycin treatment in combination with PEITC levels that by themselves induce moderate levels of apoptosis (Figure S7). The combination

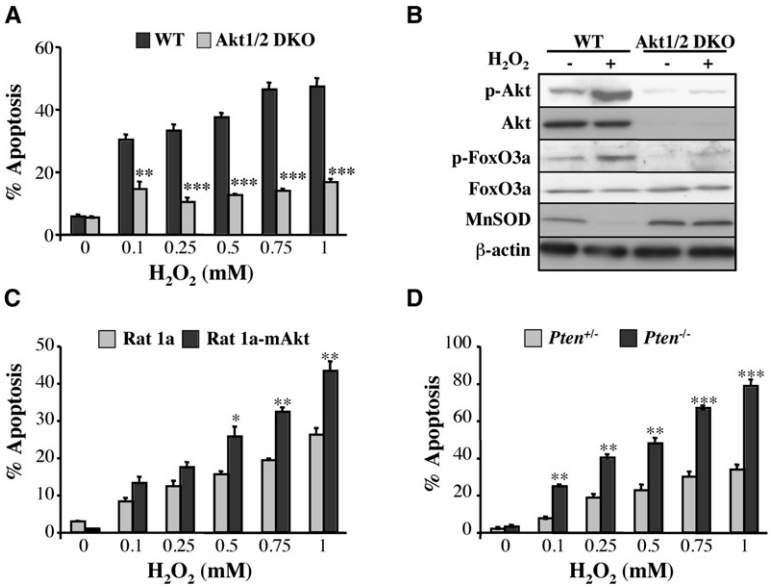


**Figure 6. Akt Sensitizes Cells to Oxidative Stress-Mediated Apoptosis in a FoxO-Dependent Manner**

(A) Akt deficiency exerts resistance to oxidative stress-induced apoptosis. DN-p53-immortalized WT and Akt1/2 DKO MEFs were treated with increasing concentrations of $H_2O_2$ (0.1–1 mM) for 2 hr, and apoptosis was quantified by DAPI staining. **p < 0.01, ***p < 0.001 versus WT.

(B) Oxidative stress increases the phosphorylation of Akt and FoxO and reduces the expression of MnSOD. DN-p53-immortalized WT and Akt1/2 DKO MEFs were treated with 500 μM $H_2O_2$ for 10 min, rinsed, and then incubated for 2 hr prior to cell lysate preparation. The immunoblot shows levels of phosphorylated Akt (Ser473) and total Akt, phosphorylated FoxO3a (Ser253) and total FoxO3a, MnSOD, and β-actin as a loading control.

(C and D) Activation of Akt sensitizes cells to $H_2O_2$-induced cell death.

(C) Apoptosis after treatment of Rat1a or Rat1a-mAkt cells with increasing concentrations of $H_2O_2$ for 2 hr. *p < 0.05, **p < 0.01 versus Rat1a.

(D) Apoptosis after treatment of *Pten*$^{+/-}$ or *Pten*$^{-/-}$ MEFs with increasing concentrations of $H_2O_2$ for 2 hr. **p < 0.01, ***p < 0.001 versus *Pten*$^{+/-}$.

Data represent the mean ± SEM of three independent experiments.

of rapamycin and PEITC significantly increased the moderate levels of apoptosis induced by 3 μM and 6 μM PEITC and was even more effective at the selective killing of both rodent and human cells with activated Akt (Figure S10). Likewise, U251 human glioblastoma cells deficient in PTEN were relatively sensitive to PEITC and PEITC plus rapamycin (Figure 7A; Figures S11A and S11B). Re-expression of WT PTEN in these cells rendered them more resistant to PEITC, whereas re-expression of mutant PTEN maintained their sensitivity (Figure 7A; Figures S11A and S11B). The selective killing of cells with activated Akt was demonstrated by using a mixed population of Rat1a cells in which only about half of the cells coexpressed activated Akt and eGFP. When exposed to PEITC plus rapamycin, most of the dead cells were GFP positive, clearly demonstrating selective killing (Figure 7B). This is consistent with the further activation of activated Akt by rapamycin (Figures S12A and S12B). Notably, rapamycin also increased the susceptibility of cells without hyperactive Akt to killing by PEITC, and this is consistent with the ability of rapamycin to activate Akt in these cells (Figure S12C).

To examine the efficacy of this strategy in cancer cells with hyperactive Akt, we used two ovarian cancer cell lines: TOV21G, in which Akt is hyperactivated even in the absence of serum, and TOV112D, in which Akt is not hyperactivated (Figure 7C). In both cell lines, rapamycin alone did not induce cell death, whereas PEITC alone induced substantially more TOV21G cell death compared with TOV112D. The combination of PEITC and rapamycin significantly increased TOV21G cell death and to some extent increased TOV112D cell death (Figure 7C; Figures S11C and S11D). This is consistent with the further activation of Akt by rapamycin in TOV21G (Figure S12B). Furthermore, knockdown of *Akt1* and *Akt2* in TOV21G cells decreased intracellular levels of ROS (Figure S13) and markedly decreased the cells' susceptibility to cell death caused by PEITC or PEITC plus rapamycin (Figure 7D). The susceptibility to apoptosis correlated with Akt activity because *Akt2* knockdown alone did not significantly decrease total Akt activity as measured by FOXO phosphorylation (Figure 7D) and also did not decrease susceptibility to apoptosis. However, knockdown of *Akt1* or both *Akt1* and *Akt2*, which markedly decreased Akt activity, also substantially decreased susceptibility to apoptosis induced by PEITC or PEITC plus rapamycin.

TOV21G cells were significantly more resistant to etoposide-induced apoptosis than TOV112D cells (Figure S14A). However, expression of activated Akt in TOV112D cells rendered them more resistant to etoposide but more sensitive to PEITC (Figures S14B and S14C). While rapamycin increased sensitivity to PEITC, it decreased sensitivity to etoposide (Figures S14A and S14B). We concluded that PEITC could be used to selectively kill cells expressing hyperactive Akt or cells treated with rapamycin due to the ability of rapamycin to activate Akt.

To verify the in vitro results in vivo, we employed xenografts of cancer cells in athymic mice. We first determined tumor growth of TOV112D and TOV112D (mAkt) cells. As shown in Figure 8A, the growth of TOV112D tumors was relatively sensitive to etoposide when compared with TOV112D (mAkt) tumors, which display an almost complete resistance to etoposide. By contrast, TOV112D (mAkt) tumors were markedly more sensitive to PEITC than TOV112D cells. We then studied the effect of PEITC and rapamycin on the growth of tumors induced by TOV21G cells (Figure 8B). Rapamycin or PEITC alone moderately attenuated the growth of the tumors. However, the combination of PEITC and rapamycin suppressed tumor growth and eradicated the tumors. Analyses of tumor sections at the endpoint of the experiment showed that PEITC alone induced profound cell death as assessed by cleaved caspase-3, whereas rapamycin alone, which elicited an increase in Akt activation, did not induce cell death but markedly inhibited BrdU incorporation (Figures 8C and 8D). At the endpoint of the experiment, no tumors were found after treatment with both PEITC and rapamycin, and therefore tumor sections were not available for analysis. We therefore analyzed tumor sections 28 days after inoculation of the cells, and it was evident that cell death, as measured by cleaved

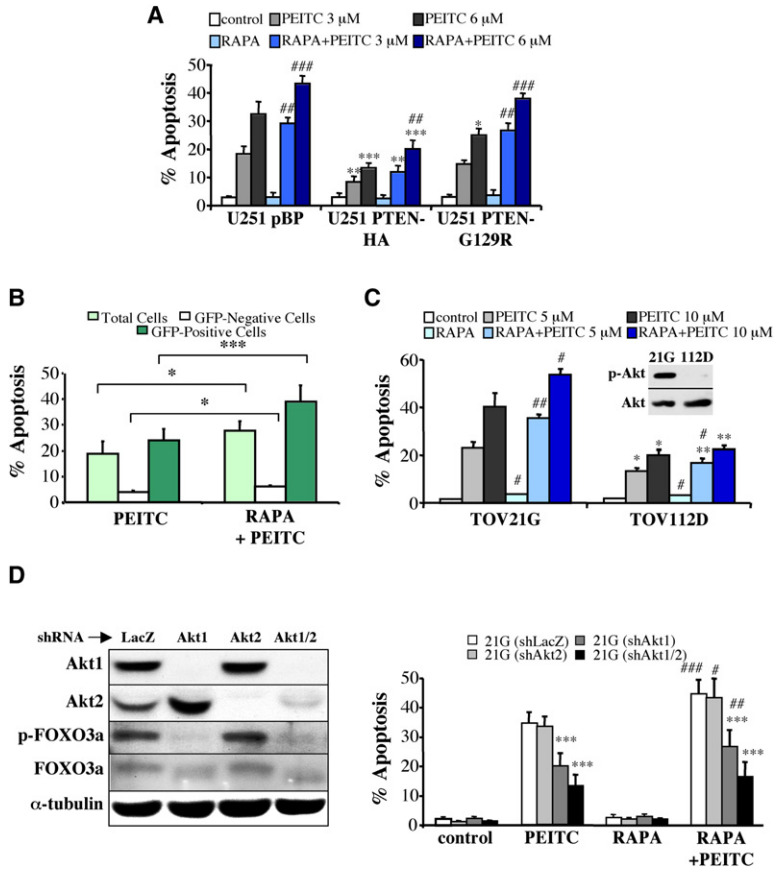


**Figure 7. Rapamycin Sensitizes Cells to PEITC-Induced Apoptosis in an Akt-Dependent Manner**

(A) PTEN-deficient U251 glioblastoma cells or U251 cells expressing G129R PTEN mutant are more sensitive to PEITC-induced apoptosis than U251 cells expressing WT PTEN. Rapamycin (RAPA) sensitizes U251 as well as U251-PTEN cells to PEITC-induced apoptosis. *p < 0.05, **p < 0.01, ***p < 0.001 versus control cells (U251 pBP); ##p < 0.01, ###p < 0.001 versus PEITC in the absence of rapamycin. Data represent the mean ± SEM of three independent experiments.

(B) Preferential killing of cells expressing activated Akt by the combination of rapamycin and PEITC. A mixed population of Rat1a (45.60% ± 1.30% of total cells) and Rat1a-mAktGFP (53.48% ± 1.33% of total cells) was treated with 6 μM PEITC for 6 hr after preincubation with 100 nM rapamycin for 3 hr. Following incubation, cells were collected and subjected to flow cytometry to assess cell death as described in Experimental Procedures. The percentage of cell death was calculated within each cell population and is presented as the mean ± SEM of at least three independent experiments. *p < 0.05, ***p < 0.001.

(C) The combination of rapamycin and PEITC preferentially induces apoptosis in ovarian cancer cells with hyperactive Akt. TOV21G and TOV112D ovarian cancer cells were preincubated with 100 nM rapamycin for 3 hr before treatment for 17 hr with 5 or 10 μM PEITC. Apoptosis was then assessed by DAPI staining. Data represent the mean ± SEM of at least three independent experiments. Inset shows an immunoblot probed with anti-phospho-Akt (Ser473) and anti-pan-Akt in a protein extract from serum-deprived TOV21G or TOV112D cells. *p < 0.05, **p < 0.01 versus TOV21G; #p < 0.05, ##p < 0.01 versus PEITC in the absence of rapamycin.

(D) Knockdown of Akt isoforms reduces the susceptibility of TOV21G cells to apoptosis induced by the combination of rapamycin and PEITC. Left: expression of Akt1, Akt2, and total Akt activity as measured by FOXO3a phosphorylation in control sh*LacZ*-, sh*Akt1*-, sh*Akt2*-, and sh*Akt1* + sh*Akt2*-expressing TOV21G cell lines. Right: quantification of apoptosis induced by rapamycin + PEITC in the different knocked-down cells, presented as the mean ± SEM of at least three independent experiments. ***p < 0.001 versus TOV21G (sh*LacZ*); #p < 0.05, ##p < 0.01, ###p < 0.001 versus PEITC in the absence of rapamycin.

caspase-3, was profoundly higher after administration of both PEITC and rapamycin than after administration of PEITC alone (Figure 8D). Thus, these results recapitulate our in vitro observations in vivo and reinforce the notion that rapamycin alone is mostly cytostatic, whereas PEITC inhibits tumor growth by eliciting cell death, overriding the resistance to cell death mediated by activated Akt. In these studies, we could not compare TOV21G cells to TOV21G cells in which Akt genes were knocked down because the latter could not form tumors within the time frame of the experiment. Collectively, these results provide a proof of concept in vivo that cell death induced by oxidative stress can selectively attenuate growth of tumor cells with hyperactivated Akt, and that the combination of oxidative stress and rapamycin could be an effective strategy to selectively eradicate tumors that display hyperactive Akt.

## DISCUSSION

We show here that Akt deficiency inhibits replicative and premature senescence induced by oxidative stress and activated Ras, whereas Akt activation induces premature senescence. The effect of Akt on cellular senescence is mediated by intracellular ROS. Akt elevates ROS levels by two mechanisms. First, the increase in oxygen consumption by Akt also increases ROS generation. Second, Akt impairs ROS scavenging by inhibiting FoxO transcription factors. FoxOs decrease ROS and inhibit cellular senescence, while the deficiency of FoxOs increases ROS and cellular senescence. The role of Akt and FoxO in cellular senescence can be extended to human cells because although telomerase activity is a major determinant of human cell life span, oxygen consumption also appears to play a role in their life span in culture (Packer and Fuehr, 1977). Indeed, we showed that HDFs deficient in Akt have an extended life span in culture and are more resistant to oxidative stress-induced senescence. Therefore, at least at the cellular level, the role of Akt and FoxO in regulating life span is conserved in mammals. Moreover, in addition to ROS scavengers known to be regulated by FoxOs, we found that FoxO1 elevates the expression of Sesn3, which has been shown to reduce intracellular ROS levels by regenerating overoxidized peroxiredoxins that deoxidize ROS (Budanov et al., 2004). Consistently, Sesn3 levels were elevated in Akt1/2 DKO MEFs, and the reduction of Sesn3 levels in these cells increased intracellular ROS to a level similar to that observed in WT cells (Figures 3G–3J). These results suggest that Sesn3 is a major determinant of ROS levels regulated by FoxO and Akt.

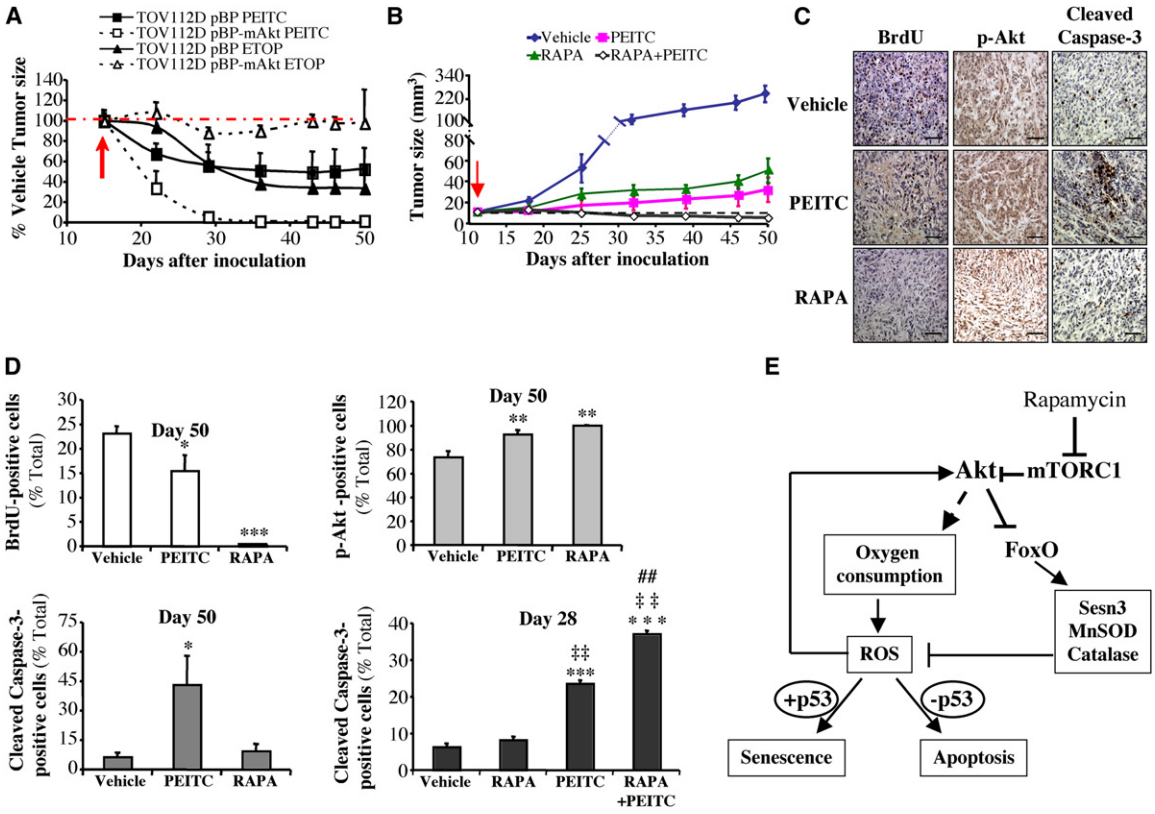


**Figure 8. In Vivo Therapeutic Activities of PEITC and PEITC Combined with Rapamycin**

(A) In vivo therapeutic activity of PEITC compared to etoposide (ETOP) in mice inoculated with TOV112D ovarian cancer cells or TOV112D (mAkt) cells. Forty-two nude mice were injected subcutaneously on both left and right flanks with TOV112D or TOV112D (mAkt) cells and randomly divided into three groups per cell line (14 mice per group, 28 tumors per group) for treatment with PEITC, etoposide, or solvent control. Graph presents the growth of tumor size for the respective treatments relative to in control mice. Red arrow indicates the start of treatment (day 13 postinoculation with tumor cells).

(B) In vivo therapeutic effect of rapamycin + PEITC in mice inoculated with TOV21G ovarian cancer cells. Thirty-six nude mice were injected subcutaneously on both left and right flanks with TOV21G cells and randomly divided into four groups (9 mice per group, 18 tumors per group) for treatment with PEITC, rapamycin, combination of rapamycin + PEITC, or solvent control. Graph presents tumor growth rate in each group. Red arrow indicates the start of treatment (day 13 post-inoculation with tumor cells). Data in (A) and (B) represent the mean ± SEM of three independent experiments.

(C) Cross-sections of tumors collected from the experiment described in (B). At day 50 postinoculation with tumor cells, cross-sections of tumors were subjected to BrdU staining (left), staining with anti-phospho-Akt (middle), and staining with anti-cleaved caspase-3 (right). Scale bars = 40 μm.

(D) Histograms showing quantification of the positively stained cells in (C) and of cleaved caspase-3 staining in tumor sections collected 28 days after inoculation. Results are expressed as the percentage of positively stained cells and are presented as the mean ± SEM percentage of positively stained cells of three sections from three treated mice. Stained and total cells were counted in four random fields of each section. *$p < 0.05$, **$p < 0.01$, ***$p < 0.001$ versus vehicle; ‡‡$p < 0.01$ versus rapamycin alone; ##$p < 0.01$ versus PEITC alone.

(E) Schematic summarizing the mechanisms by which Akt activation elevates ROS levels and sensitizes cells to either senescence or apoptosis. Activated Akt induces ROS by increasing oxygen consumption combined with the inhibition of FoxO transcription factors. FoxOs elevate the expression of ROS scavengers, in particular sestrin 3 (Sesn3), which is elevated in Akt-deficient cells. ROS could further activate Akt, which in turn further increases ROS levels. The elevation of ROS then sensitizes cells to either senescence or apoptosis depending on p53 status. Rapamycin, which inhibits mTORC1, further activates Akt as consequence of the negative regulatory loop inhibition.

A similar paradigm exists in response to lethal doses of oxidants. While Akt deficiency inhibits, Akt activation accelerates cell death induced by ROS, and the activation of FoxO inhibits this cell death. These results are consistent with the observation that hematopoietic stem cells in FoxO-deficient mice are sensitive to oxidative stress (Tothova et al., 2007). Although ROS can also induce necrotic cell death, we found that under our conditions, most of the cells died by apoptosis as assessed by nuclear condensation and fragmentation. The mechanisms by which activated Akt induces ROS, which in turn sensitize cells to either senescence or apoptosis, are summarized schematically in Figure 8E.

## The Role of Akt in Energy Metabolism—Pro- and Anticancer

The effect of Akt on tumorigenesis could be mediated through its effect on energy metabolism (Robey and Hay, 2006). Here we showed that Akt activation increases ROS levels, partially via its role in energy metabolism. The increase in ROS levels mediated by Akt could contribute to tumorigenesis by increasing mutation rate and genetic instability. However, at the same time, this also could be a barrier to tumorigenesis because an increase in intracellular ROS levels mediated by Akt renders cells more susceptible to premature senescence unless they acquire an immortalizing mutation such as p53 dysfunction. Cells in which

*Pten* is deleted are also more susceptible to premature senescence, and therefore the deletion of *p53* markedly increases tumorigenesis mediated by the deletion of *Pten* (Chen et al., 2005). Our results suggest that the senescence induced by *Pten* deletion is likely due to the activation of Akt and the increase in intracellular ROS.

Because elevated levels of ROS increase Akt activity (Figure 6B), it is possible that Akt could induce a vicious cycle of further and sustained Akt activation concomitant with a sustained increase in intracellular ROS levels, and therefore a sustained increase in a mutation rate. If cells escape the barrier of senescence, this could be a major contributing factor for tumorigenicity induced by Akt activation. However, here again this contribution of Akt to tumorigenesis is also its Achilles' heel. Despite the ability of activated Akt to inhibit apoptosis induced by a variety of apoptotic stimuli, it cannot protect against lethal doses of ROS, and this could be exploited for cancer therapy.

It was previously shown that oxidative stress can induce selective killing of cells expressing Bcr-Abl or activated Ras (Trachootham et al., 2006). However, because of the antiapoptotic activity of Akt, it was not predicted that activation of Akt also sensitizes cells to oxidative stress-induced cell death. In fact, our results suggest that Akt activation by Ras is likely the reason why cells expressing activated Ras are sensitized to killing by oxidative stress. This might also apply to Bcr-Abl, because Bcr-Abl also can activate Akt (Skorski et al., 1997).

## Future Implications: A Strategy that Selectively Eradicates Cancer Cells with Activated Akt

Akt is perhaps the most frequently activated oncoprotein in human cancers. Akt is activated by multiple mechanisms, including *Pten* mutations, p110-activating mutations, Ras activation, and receptor tyrosine kinase activation (reviewed in Bhaskar and Hay, 2007; Hay, 2005). Thus, Akt is an attractive target for cancer therapy. Although we have previously provided a proof of concept that partial ablation of Akt or the deletion of *Akt1* is sufficient to impede tumor development without having other severe physiological consequences (Chen et al., 2006; Ju et al., 2007; Skeen et al., 2006), there is still a concern that ablation of Akt might lead to undesired physiological consequences such as diabetes. Thus, a strategy to selectively eradicate cancer cells with hyperactivated Akt is highly desirable. Our observation that cancer cells expressing activated Akt are selectively killed by oxidative stress circumvents this concern. Furthermore, our results show that rapamycin treatment, which by itself is only cytostatic, also increases Akt activity, which in turn increases resistance to etoposide but further sensitizes cells to oxidative stress-induced apoptosis.

We have provided a proof of concept for this strategy in vivo in a xenograft model by showing that the combination of the ROS inducer PEITC and rapamycin can completely eradicate the growth of tumors in which Akt is hyperactivated. Furthermore, we showed that tumors expressing activated Akt are more resistant to etoposide but more sensitive to PEITC than tumors that do not express activated Akt. We did not intend to determine an exact regimen for this strategy, but we found that, at least at the cellular level, the ROS inducer 2-methoxyestradiol (2-ME) (Hileman et al., 2004), which is currently being used in clinical trials, is also effective in the selective killing of cells with hyperactivated Akt (Figure S15). Thus, this strategy could not only eliminate the concern that rapamycin treatment activates Akt but also take advantage of this phenomenon to selectively eradicate rapamycin-treated cancer cells. The combination of rapamycin and oxidative stress could be an attractive general strategy for cancer therapy, not necessarily only for cancer cells with hyperactivated Akt, particularly since rapamycin analogs are already being used in advanced stages of clinical trials.

## EXPERIMENTAL PROCEDURES

### Cells and Viruses

Primary MEFs were harvested from E13.5 embryos as described previously (Skeen et al., 2006). Experiments using primary cells were performed no later than passage 3. Experiments were also performed on WT, *Akt1/2* $^{-/-}$, *FoxO3a*$^{+/+}$, and *FoxO3a*$^{-/-}$ MEFs immortalized by DN-p53 as described previously (Skeen et al., 2006). Other cell lines used were *Pten*$^{+/-}$*p53*$^{-/-}$ and *Pten*$^{-/-}$*p53*$^{-/-}$ MEFs, Rat1a, HEK293, the glioblastoma cell line U251, and the ovarian cancer cell lines TOV112D and TOV21G. Cells were maintained in DMEM supplemented with 10% FBS. TOV112D and TOV21G cells were grown in M199/MCDB medium (1:1) with 15% FBS.

Retrovirus and lentivirus infection and generation and knockdown procedures are described in Supplemental Experimental Procedures.

### Population Doubling

Serial 3T3 cultivation was carried out as described previously (Pantoja and Serrano, 1999). Briefly, cells ($2 \times 10^5$/60 mm plate) were grown for 3 or 5 days. Cells were split every 3 or 5 days and replated at the same density ($2 \times 10^5$). This procedure was repeated for 20 passages. The increase in population doubling level (PDL) was calculated using the formula $PDL = \log(n_f/n_0)/\log 2$, where $n_0$ is the initial number of cells and $n_f$ is the final number of cells. Data were expressed as cumulated PDL from three independent experiments using three pairs of MEFs.

### SA-β-Gal Staining

Cells were plated at low density (8000 cells/35 mm plate), fixed, and stained for SA-β-Gal as described in Dimri et al. (1995) and Serrano et al. (1997) at different time points as indicated.

### BrdU Labeling

To determine actively replicating cells, BrdU incorporation assays were performed as described in Skeen et al. (2006).

### Oxygen Consumption Assay

For oxygen consumption measurement, cells were grown overnight. Cells were then harvested, washed with PBS, and resuspended in 500 μl of fresh DMEM. The rate of oxygen consumption was measured at 37°C using a Strathkelvin Model 782 oxygen meter equipped with a Clark-type oxygen electrode. Results are expressed as nanomoles of oxygen consumed per minute per million cells.

### Measurement of ROS

Intracellular ROS generation was assessed using 2′,7′-dichlorofluorescein diacetate (Molecular Probes). For details, see Supplemental Experimental Procedures.

### Western Blot Analysis

For western blot analysis, $10^6$ cells were plated in 10 cm plates and grown overnight. Whole-cell extracts were prepared in lysis buffer as described in Hahn-Windgassen et al. (2005).

### Real-Time PCR and Primers

See Supplemental Experimental Procedures.

### Hydrogen Peroxide-Induced Senescence

Primary MEFs plated at 40% confluency were treated for 2 hr with 75 μM $H_2O_2$ in DMEM containing 10% FCS (day −9). Cells were then washed, incubated in fresh medium for 7 days, and treated a second time for 2 hr with 75 μM $H_2O_2$ (day −2). Cells were then washed, incubated in fresh medium for 48 hr, and subcultured at low confluency (day 0) for up to 17 days. At days 3, 10, and 17, cells were checked for SA-β-Gal activity, BrdU incorporation, and ROS production, and cell lysates were prepared for western blotting.

### Ras-Induced Senescence

Primary MEFs ($1.5 \times 10^5$/60 mm plate) were infected with pBabe-Hygro or pBabe-Hygro-H-$Ras^{V12}$ retroviruses and selected with 150 μg/ml hygromycin for 36 hr. At the end of selection, cells were grown for 48 hr and subcultured for experiments (day 0).

### Activated Akt-Induced Senescence

Primary MEFs ($1.5 \times 10^5$/60 mm plate) were infected with pBabePuro-mAkt-ER retrovirus and selected with 2 μg/ml puromycin for 72 hr. At the end of selection, cells were allowed to grow for 48 hr and subcultured for experiments (day 0). To induce mAkt activity, cells were incubated with 300 nM 4-hydroxytamoxifen (4-OHT) for 48 hr.

### Apoptosis Assays

Cells were plated at 40% confluence, allowed to grow overnight, and then subjected to the following treatments: (1) increasing concentrations of $H_2O_2$ (100 μM to 1 mM) in DMEM for 2 hr; (2) exposure to 100 nM rapamycin for 3 hr prior to addition of $H_2O_2$; (3) exposure to PEITC as described in the figure legends; (4) exposure to 100 nM rapamycin for 3 hr prior to addition of PEITC. To quantify apoptosis, cells were then fixed for DAPI staining as described previously (Kennedy et al., 1999). PEITC/rapamycin-induced apoptosis in Rat1a-mAktGFP cells is described in Supplemental Experimental Procedures.

### Xenograft Studies

Male athymic mice (6–8 weeks old) were purchased from Charles River Laboratories. TOV21G, TOV112D, and TOV112D (mAkt) cells ($2 \times 10^6$/0.1 ml PBS) were injected subcutaneously on both left and right flanks of each mouse. Mice were equally randomized into different treatment groups (see figure legends). When tumors reached a volume of 10–15 $mm^3$, animals were treated with PEITC (35 mg/kg), rapamycin (2 mg/kg), etoposide (10 mg/kg), combination of rapamycin and PEITC (1:1), or combination of rapamycin and etoposide (1:1) as indicated from Monday to Friday by intraperitoneal injection. For further details, see Supplemental Experimental Procedures. All animal experiments were performed in accordance with the animal care policies of the University of Illinois at Chicago and were approved by the Animal Care Committee of the University of Illinois at Chicago.

### Histopathology and Immunohistochemistry

Tumors were collected at the indicated time points, rinsed in PBS, and fixed in 4% paraformaldehyde overnight. Following fixation, fixed tissues were processed and embedded in paraffin. Immunohistochemistry assays were performed as described in Chen et al. (2006). Primary antibodies included anti-cleaved caspase-3 (Asp175) and anti-phospho-Akt (Ser473) (Cell Signaling). Biotin-conjugated secondary antibody kits, avidin-biotin complexes, and diaminobenzidine were purchased from Vector Laboratories. For quantification, cells were counted from four fields at 400× magnification.

### BrdU Incorporation Assay in Mice

BrdU incorporation assays were performed as in Chen et al. (2006). Briefly, mice were injected intraperitoneally with 0.5 mg of BrdU per 10 g of body weight 2 hr prior to sacrifice.

## SUPPLEMENTAL DATA

The Supplemental Data include Supplemental Experimental Procedures, Supplemental References, and fifteen figures and can be found with this article online at http://www.cancercell.org/supplemental/S1535-6108(08)00370-X.

## ACKNOWLEDGMENTS

We would like to thank B. Knudsen (Fred Hutchinson Cancer Research Center) for the TOV-112D and TOV-21G cell lines and for sharing unpublished data. We would also like to thank Y. Luo for technical assistance and P. Bhaskar and D. Sunararajan for discussions, comments on the manuscript, and reagents. We also thank N. Chandel for advice. These studies were supported by NIH grants CA090764, AG016927, and AG025953 to N.H. and ACS-IL grant 06-24 to Y.P.

Received: March 23, 2008
Revised: October 31, 2008
Accepted: November 5, 2008
Published: December 8, 2008

## REFERENCES

Balaban, R.S., Nemoto, S., and Finkel, T. (2005). Mitochondria, oxidants, and aging. Cell *120*, 483–495.

Bhaskar, P.T., and Hay, N. (2007). The two TORCs and Akt. Dev. Cell *12*, 487–502.

Budanov, A.V., Shoshani, T., Faerman, A., Zelin, E., Kamer, I., Kalinski, H., Gorodin, S., Fishman, A., Chajut, A., Einat, P., et al. (2002). Identification of a novel stress-responsive gene Hi95 involved in regulation of cell viability. Oncogene *21*, 6017–6031.

Budanov, A.V., Sablina, A.A., Feinstein, E., Koonin, E.V., and Chumakov, P.M. (2004). Regeneration of peroxiredoxins by p53-regulated sestrins, homologs of bacterial AhpD. Science *304*, 596–600.

Chance, B., Sies, H., and Boveris, A. (1979). Hydroperoxide metabolism in mammalian organs. Physiol. Rev. *59*, 527–605.

Chen, M.L., Xu, P.Z., Peng, X., Chen, W.S., Guzman, G., Yang, X., Di Cristofano, A., Pandolfi, P.P., and Hay, N. (2006). The deficiency of Akt1 is sufficient to suppress tumor development in Pten+/− mice. Genes Dev. *20*, 1569–1574.

Chen, Z., Trotman, L.C., Shaffer, D., Lin, H.K., Dotan, Z.A., Niki, M., Koutcher, J.A., Scher, H.I., Ludwig, T., Gerald, W., et al. (2005). Crucial role of p53-dependent cellular senescence in suppression of Pten-deficient tumorigenesis. Nature *436*, 725–730.

Dimri, G.P., Lee, X., Basile, G., Acosta, M., Scott, G., Roskelley, C., Medrano, E.E., Linskens, M., Rubelj, I., Pereira-Smith, O., et al. (1995). A biomarker that identifies senescent human cells in culture and in aging skin in vivo. Proc. Natl. Acad. Sci. USA *92*, 9363–9367.

Gottlob, K., Majewski, N., Kennedy, S., Kandel, E., Robey, R.B., and Hay, N. (2001). Inhibition of early apoptotic events by Akt/PKB is dependent on the first committed step of glycolysis and mitochondrial hexokinase. Genes Dev. *15*, 1406–1418.

Greer, E.L., and Brunet, A. (2005). FOXO transcription factors at the interface between longevity and tumor suppression. Oncogene *24*, 7410–7425.

Hahn-Windgassen, A., Nogueira, V., Chen, C.C., Skeen, J.E., Sonenberg, N., and Hay, N. (2005). Akt activates the mammalian target of rapamycin by regulating cellular ATP level and AMPK activity. J. Biol. Chem. *280*, 32081–32089.

Harrington, L.S., Findlay, G.M., and Lamb, R.F. (2005). Restraining PI3K: mTOR signalling goes back to the membrane. Trends Biochem. Sci. *30*, 35–42.

Hay, N. (2005). The Akt-mTOR tango and its relevance to cancer. Cancer Cell *8*, 179–183.

Hileman, E.O., Liu, J., Albitar, M., Keating, M.J., and Huang, P. (2004). Intrinsic oxidative stress in cancer cells: a biochemical basis for therapeutic selectivity. Cancer Chemother. Pharmacol. *53*, 209–219.

Ju, X., Katiyar, S., Wang, C., Liu, M., Jiao, X., Li, S., Zhou, J., Turner, J., Lisanti, M.P., Russell, R.G., et al. (2007). Akt1 governs breast cancer progression in vivo. Proc. Natl. Acad. Sci. USA *104*, 7438–7443.

Kandel, E.S., Skeen, J., Majewski, N., Di Cristofano, A., Pandolfi, P.P., Feliciano, C.S., Gartel, A., and Hay, N. (2002). Activation of Akt/protein kinase B overcomes a G(2)/m cell cycle checkpoint induced by DNA damage. Mol. Cell. Biol. *22*, 7831–7841.

Kennedy, S.G., Kandel, E.S., Cross, T.K., and Hay, N. (1999). Akt/Protein kinase B inhibits cell death by preventing the release of cytochrome c from mitochondria. Mol. Cell. Biol. *19*, 5800–5810.

Kopnin, P.B., Agapova, L.S., Kopnin, B.P., and Chumakov, P.M. (2007). Repression of sestrin family genes contributes to oncogenic Ras-induced reactive oxygen species up-regulation and genetic instability. Cancer Res. *67*, 4671–4678.

Kops, G.J., Dansen, T.B., Polderman, P.E., Saarloos, I., Wirtz, K.W., Coffer, P.J., Huang, T.T., Bos, J.L., Medema, R.H., and Burgering, B.M. (2002). Forkhead transcription factor FOXO3a protects quiescent cells from oxidative stress. Nature *419*, 316–321.

Lee, A.C., Fenster, B.E., Ito, H., Takeda, K., Bae, N.S., Hirai, T., Yu, Z.X., Ferrans, V.J., Howard, B.H., and Finkel, T. (1999). Ras proteins induce senescence by altering the intracellular levels of reactive oxygen species. J. Biol. Chem. *274*, 7936–7940.

Leslie, N.R., Bennett, D., Lindsay, Y.E., Stewart, H., Gray, A., and Downes, C.P. (2003). Redox regulation of PI 3-kinase signalling via inactivation of PTEN. EMBO J. *22*, 5501–5510.

Matheu, A., Maraver, A., Klatt, P., Flores, I., Garcia-Cao, I., Borras, C., Flores, J.M., Vina, J., Blasco, M.A., and Serrano, M. (2007). Delayed ageing through damage protection by the Arf/p53 pathway. Nature *448*, 375–379.

Nemoto, S., and Finkel, T. (2002). Redox regulation of forkhead proteins through a p66shc-dependent signaling pathway. Science *295*, 2450–2452.

Packer, L., and Fuehr, K. (1977). Low oxygen concentration extends the lifespan of cultured human diploid cells. Nature *267*, 423–425.

Pantoja, C., and Serrano, M. (1999). Murine fibroblasts lacking p21 undergo senescence and are resistant to transformation by oncogenic Ras. Oncogene *18*, 4974–4982.

Parrinello, S., Samper, E., Krtolica, A., Goldstein, J., Melov, S., and Campisi, J. (2003). Oxygen sensitivity severely limits the replicative lifespan of murine fibroblasts. Nat. Cell Biol. *5*, 741–747.

Plas, D.R., and Thompson, C.B. (2005). Akt-dependent transformation: there is more to growth than just surviving. Oncogene *24*, 7435–7442.

Robey, R.B., and Hay, N. (2006). Mitochondrial hexokinases, novel mediators of the antiapoptotic effects of growth factors and Akt. Oncogene *25*, 4683–4696.

Rossignol, R., Gilkerson, R., Aggeler, R., Yamagata, K., Remington, S.J., and Capaldi, R.A. (2004). Energy substrate modulates mitochondrial structure and oxidative capacity in cancer cells. Cancer Res. *64*, 985–993.

Sablina, A.A., Budanov, A.V., Ilyinskaya, G.V., Agapova, L.S., Kravchenko, J.E., and Chumakov, P.M. (2005). The antioxidant function of the p53 tumor suppressor. Nat. Med. *11*, 1306–1313.

Schmitt, C.A. (2007). Cellular senescence and cancer treatment. Biochim. Biophys. Acta *1775*, 5–20.

Serrano, M., Lin, A.W., McCurrach, M.E., Beach, D., and Lowe, S.W. (1997). Oncogenic ras provokes premature cell senescence associated with accumulation of p53 and p16INK4a. Cell *88*, 593–602.

Skeen, J.E., Bhaskar, P.T., Chen, C.C., Chen, W.S., Peng, X.D., Nogueira, V., Hahn-Windgassen, A., Kiyokawa, H., and Hay, N. (2006). Akt deficiency impairs normal cell proliferation and suppresses oncogenesis in a p53-independent and mTORC1-dependent manner. Cancer Cell *10*, 269–280.

Skorski, T., Bellacosa, A., Nieborowska-Skorska, M., Majewski, M., Martinez, R., Choi, J.K., Trotta, R., Wlodarski, P., Perrotti, D., Chan, T.O., et al. (1997). Transformation of hematopoietic cells by BCR/ABL requires activation of a PI-3k/Akt-dependent pathway. EMBO J. *16*, 6151–6161.

Tothova, Z., Kollipara, R., Huntly, B.J., Lee, B.H., Castrillon, D.H., Cullen, D.E., McDowell, E.P., Lazo-Kallanian, S., Williams, I.R., Sears, C., et al. (2007). FoxOs are critical mediators of hematopoietic stem cell resistance to physiologic oxidative stress. Cell *128*, 325–339.

Trachootham, D., Zhou, Y., Zhang, H., Demizu, Y., Chen, Z., Pelicano, H., Chiao, P.J., Achanta, G., Arlinghaus, R.B., Liu, J., and Huang, P. (2006). Selective killing of oncogenically transformed cells through a ROS-mediated mechanism by beta-phenylethyl isothiocyanate. Cancer Cell *10*, 241–252.

Warburg, O., Geissler, A.W., and Lorenz, S. (1967). [On growth of cancer cells in media in which glucose is replaced by galactose.] Hoppe Seylers Z. Physiol. Chem. *348*, 1686–1687.

Yu, R., Mandlekar, S., Harvey, K.J., Ucker, D.S., and Kong, A.N. (1998). Chemopreventive isothiocyanates induce apoptosis and caspase-3-like protease activity. Cancer Res. *58*, 402–408.